Template for manuscript

Author One[1], **Author Two**[1], **Author Three**[2,3], **and Author Four**[1]

[1]**Author one affiliation**
[2]**Author two affiliation**
[3]**Author three affiliation**

Corresponding author:
Author Four[1]

Email address: email@address

ABSTRACT

This is the abstract.

Keywords: Keyword1; Keyword2; Keyword3

INTRODUCTION

...

MATERIALS AND METHODS

...

RESULTS

...

DISCUSSION

...

CONCLUSIONS

...

AUTHOR CONTRIBUTIONS

...

INSTITUTIONAL REVIEW

...

DATA AVAILABILITY

...

FUNDING

...

ACKNOWLEDGMENTS

...

CONFLICTS OF INTEREST

...

REFERENCES

Britton, C. and Dodd, J. (1976). Relationships of photosynthetically active radiation and shortwave irradiance. *Agricultural Meteorology*, 17(1):1–7.

Fausto, R. S., van As, D., Mankoff, K. D., Vandecrux, B., Citterio, M., Ahlstrom, A. P., Andersen, S. B., Colgan, W., Karlsson, N. B., Kjeldsen, K. K., Korsgaard, N. J., Larsen, S. H., Nielsen, S., Pedersen, A. O., Shields, C. L., Solgaard, A. M., and Box, J. E. (2021). Programme for monitoring of the greenland ice sheet (promice) automatic weather station data. *Earth System Science Data*, 13(8):3819–3845.

Holtgrieve, G. W., Schindler, D. E., Branch, T. A., and A'mar, Z. T. (2010). Simultaneous quantification of aquatic ecosystem metabolism and reaeration using a bayesian statistical model of oxygen dynamics. *Limnology and Oceanography*, 55(3):1047–1063.

How, P., Abermann, J., Ahlstrom, A., Andersen, S., Box, J. E., Citterio, M., Colgan, W., Fausto., R., Karlsson, N., Jakobsen, J., Langley, K., Larsen, S., Lund, M., Mankoff, K., Pedersen, A., Rutishauser, A., Shield, C., Solgaard, A., Van As, D., Vandecrux, B., and Wright, P. (2022). Promice and gc-net automated weather station data in greenland. url: https://dataverse.geus.dk/citation?persistentId=doi:10.22008/FK2/IW73UU.

Lürig, M. D., Narwani, A., Penson, H., Wehrli, B., Spaak, P., and Matthews, B. (2021). Non-additive effects of foundation species determine the response of aquatic ecosystems to nutrient perturbation. *Ecology*, 102(7).

Moritz, S. and Bartz-Beielstein, T. (2017). imputeTS: Time Series Missing Value Imputation in R. *The R Journal*, 9(1):207–218.

R Core Team (2024). *R: A Language and Environment for Statistical Computing*. R Foundation for Statistical Computing, Vienna, Austria.

Vachon, D. and Prairie, Y. T. (2013). The ecosystem size and shape dependence of gas transfer velocity versus wind speed relationships in lakes. *Canadian Journal of Fisheries and Aquatic Sciences*, 70(12):1757–1764.

Winslow, L. A., Zwart, J. A., Batt, R. D., Dugan, H. A., Woolway, R. I., Corman, J. R., and Read, J. S. (2016). Lakemetabolizer: An r package for estimating lake metabolism from free-water oxygen using diverse statistical models. *Inland Waters*, 6(4).

APPENDIX

0.1 Study design and setup

In 2019, 12 glacial lakes ($N = 12$) were chosen for an experiment near Narsarsuaq, Greenland (61.1567°N, -45.4254°E). These glacial lakes vary in area (0.21 to 1.82 hectares) and maximum depth (2 to 8 m), but are all clustered within a few kilometers of each other. All lakes were fishless at the beginning of the experiment. Six lakes were subsequently introduced with three-spined sticklebacks (*Gasterosteus aculeatus*) from nearby lakes. Lake B1P1, B2P2, and B3P3 were introduced with *Gasterosteus aculeatus* from a single population (lake L26, 61.253333°N, -45.529141°E), while lake B2P3, B3P1, and B3P2 were introduced with *Gasterosteus aculeatus* from two populations (lake L26, 61.253333°N, -45.529141°E and lake ERL33, 61.118369°N, -45.580845°E). The remaining six lakes B1P4, B2P4, B3P0, ERL85, ERL122, and ERL152 were used as fishless control. For the purpose of this study, the origin of the introduced *Gasterosteus aculeatus* is of minor importance, as they all originate from the same area (Supplementary Table S1).

In 2021, 2022, and 2023, all 12 lakes were monitored over several days. For that purpose, EXO2 multiparameter sondes were installed (YSI, Yellow Springs, OH, USA), tracking ecosystem parameters with high frequency (2-minute intervals in 2021 and 2022, 5-minute intervals in 2023 with the exception of ERL122, which was monitored in 15-minute intervals). For the purpose of this study, only dissolved oxygen (hereafter DO) and temperature measurements yielded from these sondes are relevant. The sensors were situated at a water depth of approximately 1-1.5 m in each lake. All optical sensors were wiped clean before every measurement with a built-in wiper. The monitoring period was 16 September-24 September in 2021, 22 June-3 July in 2022, and 22 June-17 July in 2023.

Supplementary Table S1. Lakes included in the experiment, along with treatment and general characteristics.

Lake	Treatment	Latitude (°N)	Longitude (°E)	Altitude (m)	Area (hectare)	Maximum Depth (m)
B1P1	Fish	61.15338	-45.57081	272	0.21	4.00
B2P2	Fish	61.12299	-45.55988	255	0.50	3.00
B3P3	Fish	61.13385	-45.57556	258	0.30	5.00
B2P3	Fish	61.12275	-45.55696	261	0.41	4.25
B3P1	Fish	61.13130	-45.51195	180	0.40	2.00
B3P2	Fish	61.12788	-45.51031	201	0.53	4.50
B1P4	No Fish	61.16552	-45.56801	304	0.44	2.20
B2P4	No Fish	61.12192	-45.55497	261	0.51	7.00
B3P0	No Fish	61.13210	-45.51416	177	0.81	4.00
ERL85	No Fish	61.14171	-45.59328	120	1.82	8.00
ERL122	No Fish	61.14182	-45.53623	111	1.10	5.00
ERL152	No Fish	61.14646	-45.59235	156	0.73	4.50

0.2 Data sources

DO ($mg\,L^{-1}$) and water temperature ($°C$) measurements were yielded from EXO2 multiparameter sondes, as described in section Study design and setup. For the purpose of estimating ecosystem metabolism, wind and irradiation data were yielded from the Programme for Monitoring of the Greenland Ice Sheet (PROMICE), providing automatic weather station data (Fausto et al., 2021). The dataset named `QAS_L_hour.csv` originating from the QAS_L automated weather station near Narsarsuaq was downloaded from a public database provided by PROMICE (How et al., 2022). Wind data was provided as average wind speed in hourly intervals ($m\,s^{-1}$), while irradiation was provided as downwelling shortwave irradiation additionally corrected for the tilt of the sensor ($W\,m^{-2}$).

0.3 Data pipeline

The data preparation and analysis for estimating lake metabolism was done separately for each monitoring period (16 September-24 September 2021, 22 June-3 July 2022, and 22 June-17 July 2023).

First, the raw sonde data from each lake were imported and merged into one dataset for a given monitoring period. The variables required for lake metabolism estimation were water temperature and DO. Next, an outlier analysis was performed by removing values higher than three times the median absolute deviation of all values in a sliding window of one day window size (Lürig et al., 2021). After outlier removal, the time series of water temperature and DO were plotted and subsequently investigated for larger data gaps due to potential lack of sensor measurements over certain periods.

To ensure overlapping estimation of lake metabolism, the data was subsequently cut to achieve equal starting and ending time points for all lakes during a given monitoring period. Due to large data gaps during the period of 2022, we chose to keep as much complete days as possible in order to estimate the maximum amount of days, rather than selecting the longest common monitoring period for all lakes.

After cutting the sonde data, they were subsequently merged with the weather data. Since the weather data were collected in hourly intervals, they were inflated to match the measurement intervals of the sonde data (see section Study design and setup).

After merging sonde and weather data, potential missing values due to outlier removal were imputed by a weighted moving average, where the weights of observations around the central value to be imputed decrease exponentially (Moritz and Bartz-Beielstein, 2017). For larger data gaps spanning over several hours (due to sonde malfunction rather than outlier removal), we chose to not estimate lake metabolism for the affected days.

All data preparation and analysis was done with the `R` programming language (R Core Team, 2024). To estimate lake metabolism, the package `LakeMetabolizer` was used (Winslow et al., 2016). Specifically, a Bayesian framework to estimate whole lake metabolism from free-water DO by using the function `metab.bayesian` was chosen for this analysis (Holtgrieve et al., 2010). In order to be able to fit the model, a minimum of 6 variables are needed as input:

1. doobs: DO concentration measurements ($mg\,L^{-1}$)
2. do.sat: Equilibrium DO concentration for specific temperature ($mg\,L^{-1}$, hereafter do.sat)
3. k.gas: Gas and temperature specific gas transfer coefficient (m^{-1}, hereafter k.gas)
4. par: Photosynthetically active radiation ($\mu mol\,m^{-2}\,s^{-1}$, hereafter par)
5. z.mix: Actively mixed layer depth (m, hereafter z.mix)
6. wtr: Water temperature ($°C$)

Some of the variables listed above have to be derived from other time series data prior to estimating lake metabolism, namely do.sat, k.gas, par, and z.mix. The necessary functions are provided by the `LakeMetabolizer` package. do.sat was derived by using the function `o2.at.sat`, which calculates the equilibrium DO concentration in water at supplied conditions. To estimate k.gas, a gas transfer coefficient model must be fit. The `LakeMetabolizer` package offers different methods, and we chose an empirical wind-based gas exchange model, introduced by Vachon and Prairie in 2013 (Vachon and Prairie, 2013). This model not only takes wind into consideration, but also lake area, and is implemented in the function `k.vachon`. Notably, wind speed has to be normalized to 10 m sensor height before fitting any gas exchange model, which is achieved with the function `wind.scale`. All models of gas exchange return a k_{600} value, a gas exchange normalized to a Schmidt number (Sc) of 600, or O_2 at 17.5 $°C$. After estimating k_{600}, it must be transformed to k.gas by using the function `k600.2.kGAS`. par was derived from shortwave irradiation, which we had available (see section Data sources). To achieve this transformation, we used the function `sw.to.par`, which uses the simple empirical transformation $par = 2.114 \times sw$ (Britton and Dodd, 1976). To estimate z.mix, one normally needs a time series profile of water temperature or water density. Since we did not have such data available, we decided to simulate actively mixed layer depth by drawing from a

uniform distribution with limits 0 and maximum depth of the lake. The reasoning behind this simulation is that, although the simulated time series of z.mix likely differing substantially from the actual, a possible treatment effect of fish versus no fish should still be consistent, given the simulation is performed equally in all lakes.

After performing the data preparation and the derivation for certain model inputs, the Bayesian lake metabolism model was fitted for each lake and monitoring period. The Bayesian model is special, as it considers 2 types of errors: Differences between the true data generating process and the process defined in the model (process error) and errors resulting from inaccuracies of DO measurements (observation error). Reflecting this philosophy, the Bayesian model distinguishes between 3 categories of DO values: y represents the DO measurements, α the true but unknown DO values, and α^* the model's estimates of the true value. The observed DO measurements y are modeled as random deviations from the true value α:

$$y_t \sim N(\alpha_t, \tau_v), \tag{1}$$

where τ_v is the precision of the observation error (precision is the reciprocal of variance). Note, that the Bayesian model fits parameter values by making a comparison between observed and theoretical values of DO. This comparison is made in equation 2, where we define the true value of DO at time t, α_t, as being normally distributed with mean α_t^* and process precision τ_w:

$$\alpha_t \sim N(\alpha_t^*, \tau_w), \tag{2}$$

where τ_w is the precision of the process error. The important distinction of process and observation error is that process error affects the state of the system at time $t+k (k = 0, 1, ..., T-t)$, because the state evolves dynamically, whereas observation error only affects the state of the system at time t.

Both τ_v and τ_w are given minimally informative priors following a gamma distribution with shape and rate parameters of 0.001.

The Bayesian model can be described by the following equations:

$$\alpha_t^* = \begin{cases} \alpha_{t-1} + \alpha_t & \text{if } k_t = 0, \\ \frac{\alpha_t}{k_{t-1}} + \frac{-\exp(-k_{t-1})\alpha_t}{k_{t-1}} + \exp(-k_{t-1})\alpha_{t-1} & \text{otherwise,} \end{cases} \tag{3}$$

$$\alpha_t = \mathbf{X}_{t-1}\boldsymbol{\beta} + k_{t-1}O_{s,t-1}, \tag{4}$$

$$k_t = \frac{K_t^* \Delta t}{z_t}. \tag{5}$$

In this equation structure, k_t is the coefficient of gas exchange; $\mathbf{X}$ is an $n \times 2$ matrix of predictor variables with I (irradiation in arbitrary light units) in the first column and $\ln T$ ($^\circ C$) in the second column; $\boldsymbol{\beta}$ is a 2×1 vector of parameters to be estimated (ι, ρ). ι represents the parameter for Gross Primary Production (hereafter GPP), implying a linear relationship between GPP and irradiation, and ρ represents the parameter for Respiration (hereafter R), implying a log-linear relationship between R and temperature; O_s is the equilibrium DO concentration at supplied conditions; K_t^* is a stochastic node, with $K_t^* \sim N(K_t, \sigma_k)$, where K_t is the gas exchange coefficient, and σ_k the precision thereof; the default precision is $1/(0.1 \times K_t)$; finally, z_t is the mixed layer depth.

From equation 3, we can see that if $k_t = 0$ (i.e., no gas exchange with the atmosphere), the oxygen levels in the water are modeled to be additive for each time step. Furthermore, we can see that the gas exchange coefficient is dependent on mixed layer depth (equation 5).

While the estimate of gas exchange coefficient serves as prior information for K, priors for the fitted GPP and R parameters (ι and ρ) can also be defined. The default priors for ι and ρ are normal distributions with mean 0 and variance 1×10^5 ($\iota_t \sim N(0, 10^5)$, $\rho_t \sim N(0, 10^5)$) and were used in our case.

To estimate metabolism, the median of the posterior distribution of the parameters is used as a scalar estimate. Daily GPP and R estimates represent an integrated estimate of these scalars over a 24-hour window. Uncertainty of GPP and R estimates is expressed as the posterior standard deviation of the respective parameters (ι and ρ), multiplied by the square root of the corresponding covariate (I and $\ln T$). NEP is the sum of GPP and R, and the standard deviation of NEP is the sum of the standard deviations for GPP and R.

In total, 5 parameters are fit in this Bayesian model, namely ι, ρ, K, τ_v, and τ_w. For all parameters except K, (default) minimally informative priors were used. Regarding K, as described above, its estimate (from the separate gas transfer coefficient model) serves as a prior.

Estimates of the posterior distribution of the parameters were sampled using Gibbs sampling implemented in Just Another Gibbs Sampler (JAGS). Prior to running the Bayesian model, it must be installed.

0.4 Sensitivity analysis for mixed layer depth

As mentioned in section Data pipeline, we did not have the necessary data to estimate mixed layer depth. An initial approach to assess this issue was to investigate the effect of different mixed layer depths on daily metabolism estimates. For that purpose, we selected a few lakes for different monitoring periods (2021, 2022, 2023). Notably, mixed layer was held constant, which is rarely the case in reality. In Figure S1, an example of a sensitivity analysis for lake B1P1 in 2021 is depicted. Plots A-C depict the daily GPP, R, and NEP estimates for different mixed layer depths. For each mixed layer value, a separate model was fitted, holding all other covariates equal. Apparently, mixed layer depth substantially impacts respiration, where a smaller mixed layer depth is associated with higher (more negative) R. In contrast, GPP is barely affected by mixed layer depth. Plots D-H show the input variables required to fit the metabolism models, apart from mixed layer depth. Since mixed layer particularly effects daily R estimates, careful consideration with regards to overcoming this limitation is required. Notably, the effect of variation in mixed layer depth was consistent across most lakes and monitoring periods

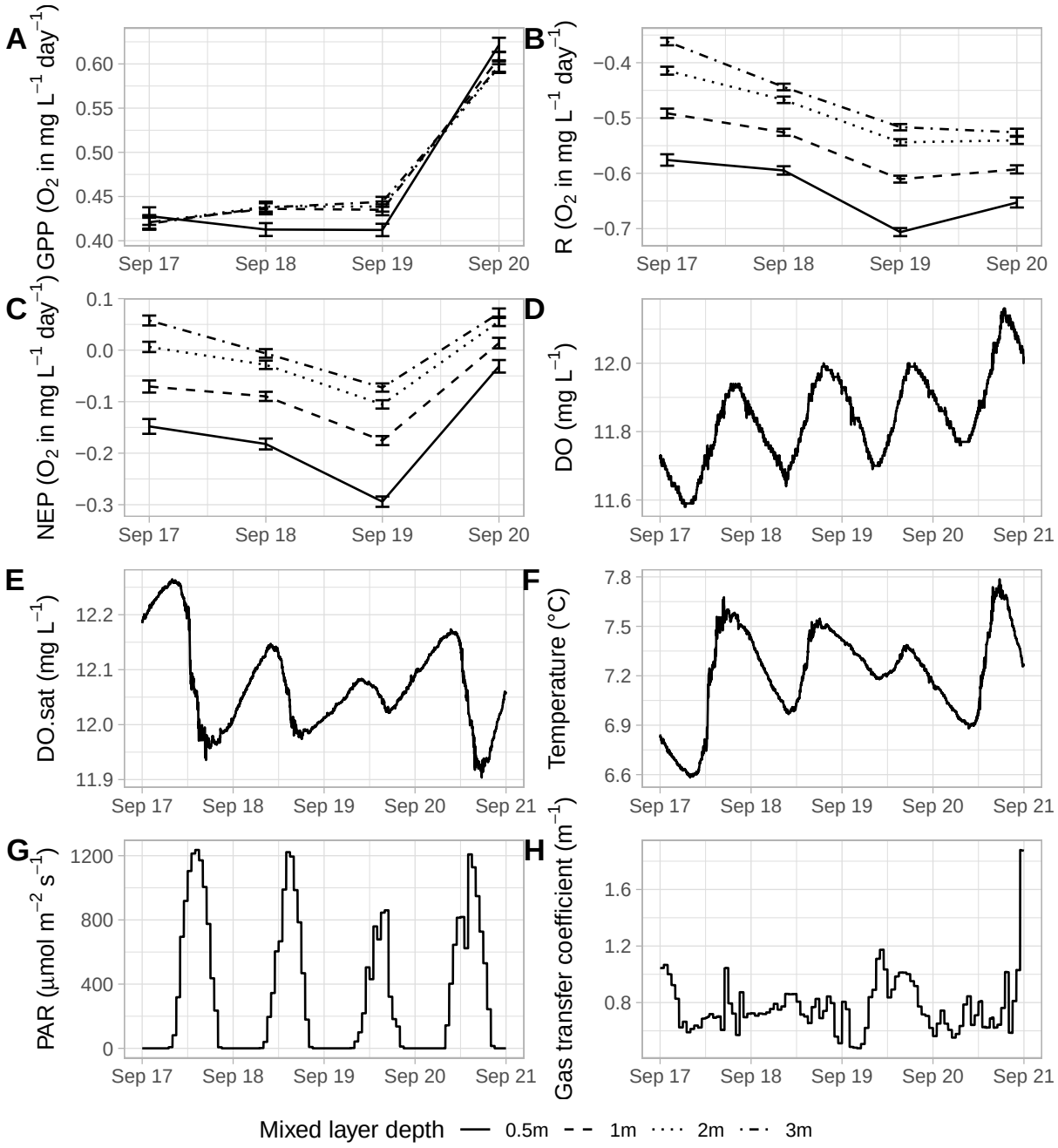

Supplementary Figure S1. Example of a sensitivity analysis for mixed layer depth in lake B1P1, 2021. Figures A-C depict GPP, R, and NEP estimates for different mixed layer depths. Figures D-H depict time series of input variables needed for metabolism estimation.